J Solid State Electrochem (2011) 15:2383–2393
DOI 10.1007/s10008-011-1494-5

ORIGINAL PAPER

Hydrogen peroxide electroreduction on composite PEDOT films with included gold nanoparticles

Veniamin V. Kondratiev · Nadezhda A. Pogulaichenko · Elena G. Tolstopjatova · Valery V. Malev

Received: 26 April 2011 / Revised: 21 June 2011 / Accepted: 22 June 2011 / Published online: 12 July 2011

Abstract Composite PEDOT/Au films were obtained by chemical deposition of dispersed gold nanoparticles into PEDOT (poly-3,4-ethylenedioxythiophene) conducting polymer matrix. Morphology of the obtained gold-containing films was studied by SEM and TEM methods. To study the kinetics of the hydrogen peroxide electroreduction that proceeds on glassy carbon electrodes modified with such films, we used phosphate buffer solutions containing addenda of hydrogen peroxide species. It was observed that the electroreduction process takes place on both the gold clusters' surface and the film surface free of metal inclusions. The rate of the process is higher in the first case and rises with increasing the gold content in modifying films, but in the limit of large gold contents it is limited only by diffusion of hydrogen peroxide species in the bathing solution. A simple theory of such parallel electroreduction is proposed, which appears to allow for quantitative treatment of the obtained results.

Keywords Nanocomposite materials · Poly-3,4-ethylenedioxythiophene · Conducting polymers · Gold nanoparticles · Cyclic voltammetry · Rotating disk electrode

V. V. Kondratiev (✉) · N. A. Pogulaichenko · E. G. Tolstopjatova · V. V. Malev
Department of Chemistry, St. Petersburg State University, Petrodvoretz, Universitetsky pr.26, 198504 St-Petersburg, Russian Federation
e-mail: vkondratiev@mail.ru

V. V. Malev
Institute of Cytology, Russian Academy of Sciences, Tikhoretsky pr. 4, 194064 St. Petersburg, Russian Federation

Introduction

Catalytic activity of metal nanoparticles and hybrid materials containing such particles has attracted much attention during the recent years due to possible applications of such objects in electrocatalysis and sensor devices. Chemical or electrochemical deposition of metal particles in conducting polymers, particularly in poly-3,4-ethylenedioxythiophene (PEDOT) films, is an appropriate way for synthesis of metal-containing polymer materials.

A great number of papers has been devoted to studies of metal-containing polymers, in particular those containing gold nanoparticles, such as poly-3,4-ethylenedioxythiophene [1–18], polyaniline [19–26], and polypyrrole [27–31]. In most studies, the synthetic approach based on the metal particles' electroreduction in polymer films or formation of such ones during syntheses from monomer-containing solutions with addition of pre-synthesized metal nanoparticles was applied. A high catalytic activity of dispersed gold particles deposited on different substrates in relation to the oxygen and hydrogen peroxide electroreduction was reported in a series of papers [25, 32–41]. However, we were not able to find any studies of the hydrogen peroxide electroreduction at PEDOT films with inclusion of gold particles (PEDOT/Au). We have therefore undertaken the corresponding study in case of glassy carbon (GC) electrode modified by PEDOT/Au film (GC/PEDOT/Au electrode) immersed into phosphate buffer solutions. This process was also chosen by us as a probe reaction for evaluating the electrochemical properties of PEDOT/Au films obtained at different conditions of their synthesis. In particular, the effect of gold loading of PEDOT films was studied in this work by measurements of voltammetric curves of H_2O_2 electroreduction on rotating disk electrode (RDE).

Experimental

PEDOT films were synthesized by electrodeposition on GC substrate under galvanostatic conditions at current density value j=1 mA cm^{-2}. The solutions used for the deposition contained 0.05 M 3,4-ethylenedioxythiophene (Aldrich), 0.5 M lithium perchlorate ($LiClO_4$, Aldrich, reagent grade) in acetonitrile purified cryogenically (HPLC grade, Cryochrom, Russia, water content below 0.05%). An average thickness of the prepared PEDOT films was about 0.3 μm, as was calculated based on the polymerization charge. During such calculations we assumed that the film density equaled 1 g cm^{-3} and 2.25 electrons are consumed on formation of one monomer unit [42]. Fabrication of PEDOT/Au composite films was performed by electroless deposition of gold from solution of 5×10^{-3} M $HAuCl_4$ in 0.1 M H_2SO_4 [9].

Potentiostat AUTOLAB PGSTAT-30 (ECO CHEMIE, Netherlands) and rotating disk electrode VED-06 (Volta Co. Ltd., Russia) were used for electrochemical measurements. The potential sweep rates in CV measurements were in the range of 10–50 mV s^{-1}. Electrochemical measurements were performed in a three-electrode glass cell using GC disk electrode (S=0.07 cm^2), platinum wire as an auxiliary electrode, and saturated silver–silver chloride electrode as a reference one. The GC disk electrode was polished to a mirror finish using alumina powder (0.05 μm) and then washed with deionized water prior to use. Electrochemical quartz crystal microbalance (EQCM) measurements were performed with QCM 100 Quartz Crystal Microbalance Analog Controller and QCM25 Crystal Oscillator (SRS, USA).

The kinetics of the H_2O_2 electroreduction was studied in phosphate buffer electrolytes, deaerated with argon at room temperature (20±2°C). Morphology of the synthesized PEDOT and PEDOT/Au films was characterized using scanning electron microscopy (SEM; SUPRA 40VP, Carl Zeiss, Germany) and transmission electron microscopy (TEM; LIBRA 200FE, Carl Zeiss, Germany) methods.

Results and discussion

Synthesis and characterization of PEDOT/Au films

Syntheses of PEDOT/Au composite films were performed by a two-step procedure consisting of the reduction of a PEDOT film in supporting electrolyte solution (0.1 M H_2SO_4) followed by its immersion into solution containing chloride complexes of gold $HAuCl_4$. As the standard electrode potential of the couple $Au(III)Cl_4^-/Au(0)$ is equal to 1.005 V [43], gold(III)-ions can act as an effective oxidant. Interactions of these ions with reduced fragments of PEDOT film cause their spontaneous oxidation and formation of metal gold particles in the film. The fact of gold particles' deposition into PEDOT films with formation of PEDOT/Au composite films was confirmed by means of energy-dispersive X-ray analysis.

The amounts of metallic gold loaded into PEDOT film were determined by EQCM measurements, as described previously in [11]. For five loadings repeated consecutively, the mass of the incorporated gold increased, as shown in Table 1. It was found that, in case of not too high gold loadings, such mass increases, Δm, were almost proportional to duration τ of exposition of a PEDOT film in the solution of Au(III) of a specified concentration. At higher loadings some deviations from such proportionality between Δm and τ occurred and the corresponding mass values obtained at these conditions were less reproducible.

Morphology of PEDOT/Au composites was studied by SEM and TEM methods. The obtained SEM images show that pristine PEDOT films have an inhomogeneous net-like structure with a large amount of pores, the sizes of which are in the range of 50–200 nm. After chemical deposition of gold (from 5×10^{-3} M $HAuCl_4$ solution, 30 s) into PEDOT film, nano-sized agglomerates of gold particles were observed on its surface as light-gray dots or spots (Fig. 1). Sizes of isolated gold particles lay in the range of 30–70 nm. A more precise estimation of the sizes of gold particles deposited into PEDOT films and their distribution within the films were performed by TEM. Figure 2 shows a typical TEM image of a PEDOT/Au sample. An irregular distribution of the particles of predominantly spherical shape with the size in the range of 40–50 nm was observed on the film surface. Agglomerates of gold particles similar to those detected by SEM (Fig. 1) were also observed on the polymer surface.

Previously we explained that in PEDOT/Pd films Pd-clusters are mainly located close to polymer fibers [44]. This indirectly evidences that centers of primary metal nucleation are located on polymer fibers, which we assume is due to pre-interactions of metal ions with sulfur atoms of thiophene rings. We believe that, in the case of PEDOT/Au composite films, the same character of the gold particles' inclusion into the films with a parallel nucleation of gold particles in polymer pores accessible for gold(III)-ions takes

Table 1 Masses (Δm) of metallic gold loaded into PEDOT film at different loading durations (τ)

№	τ (s)	Δm (μg·cm^{-2})
1	30	6.5
2	60	10.8
3	90	17.4
4	120	23.3
5	180	28.9

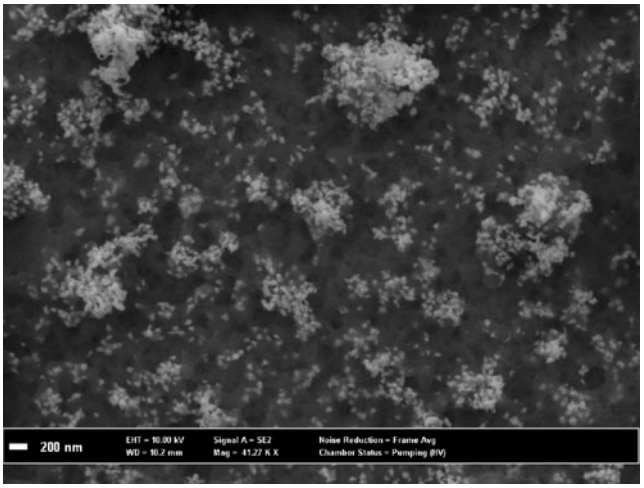

Fig. 1 Typical SEM image of composite PEDOT/Au film. Time of gold loading from a 5×10^{-3} M $HAuCl_4$+0.1 M H_2SO_4 solution was equal to 30s

place. However, both the obtained SEM- and TEM-images do not give direct evidence in favor of three-dimensional distribution of metal particles. We should also note that the sizes of gold particles and their distributions obtained by SEM and TEM methods for different samples of PEDOT/Au composites synthesized under identical conditions are in good agreement.

The images obtained for film samples with the increased duration of gold loading into PEDOT (60 s) from solutions of the same $HAuCl_4$ concentration (5×10^{-3} M) manifested appropriate increases of both the size of isolated gold particles (70–80 nm) and the density of their distribution. An increase of the number of agglomerates and formation of larger aggregates (up to 200–300 nm) were also observed in such conditions.

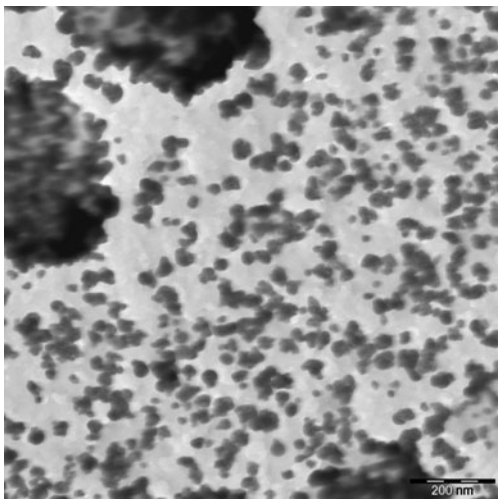

Fig. 2 Typical TEM image of composite PEDOT/Au film. Time of gold loading from a 5×10^{-3} M $HAuCl_4$+0.1 M H_2SO_4 solution was equal to 30 s

Electroreduction of hydrogen peroxide

Figure 3 shows typical voltammetric cathodic curves for pristine PEDOT film (curve 1) and composite PEDOT/Au film (curve 2) on rotating GC disk electrode in 0.2 M phosphate buffer solution (PBS; pH=6.86), and also in PBS containing $1\cdot10^{-3}$ M hydrogen peroxide (*curves 3* and *4*). Curve 5 of the figure will be discussed in more detail later; for now we only indicate that it represents a partial voltammetric curve of the hydrogen peroxide reduction on Au particles.

As can be seen from Fig. 3, in the potential range under investigation, no noticeable cathodic currents appear on the background curve of PEDOT film (curve 1) in PBS without additions of H_2O_2. At the same time, in the presence of gold particles in PEDOT film (see curve 2), a cathodic wave is observed at the electrode potentials in the range of −0.8 to −1.0 V. This wave can be attributed to the hydrogen electrogeneration on gold particles from water molecules or other proton donors (protonated phosphate ions). We will further consider this wave as a background current independently of its origin.

In case of pristine PEDOT film, substantial cathodic currents appear only after the addition of hydrogen peroxide into PBS (curve 3), and they increase dramatically in a composite film containing metallic gold (curve 4). It follows from this data that the hydrogen peroxide reduction on PEDOT/Au composite (Fig. 3, curve 4) runs not only on the surface of gold particles, but also on the surface of pristine PEDOT-modified GC electrode, although the rate of the latter process is somewhat lesser than that of the former (compare curves *3* and *4*).

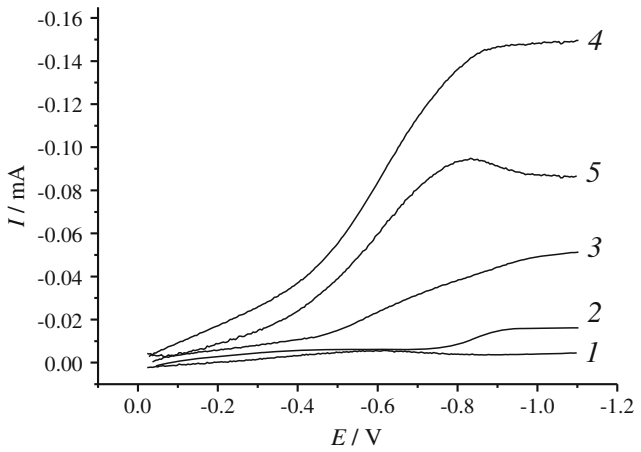

Fig. 3 RDE voltammetry curves of GC/PEDOT electrode in solution of PBS in the absence (*1*) and presence (*3*) of 0.001 M H_2O_2 and those of GC/PEDOT/Au electrode in PBS solution in the absence (*2*) and presence (*4*) of 0.001 M H_2O_2 (substrate—GC disk of 0.07 cm^2, f= 2,500 rpm, scan rate 10 mV s^{-1}). Duration of gold loading from solution of 1×10^{-3}M $HAuCl_4$+0.1 M H_2SO_4 is 60 s

The limiting cathodic current of the hydrogen peroxide reduction in case of composite PEDOT/Au film with the total amount of gold equal to 10.8 μg was approximately two to three times greater than that of the GC/PEDOT electrode in the same solution. We should also indicate that the wave of the hydrogen peroxide reduction on PEDOT/Au film noticeably shifted to more positive potentials in comparison with pristine PEDOT film. In particular, the half-wave potential of the H_2O_2 reduction on PEDOT/Au film equals −570 mV; that is about 200 mV more positive than that of pristine PEDOT film at the same conditions. Thus, the obtained results point out a significant increase of the rate of the H_2O_2 reduction in the presence of incorporated particles of dispersed gold, and, probably, electrocatalytic properties of gold particles with respect to the process under our study. As to the H_2O_2 reduction on pristine PEDOT films (and the PEDOT/Au film surface free of gold clusters), we can only indicate here that the observed limiting current of this process (see curve 3 of Fig. 3) does not result from a slow electron transfer through the film volume, since values of such current occur proportional to the hydrogen peroxide concentration in the bathing electrolyte. Now, it is not clear why the reduction proceeds at so negative electrode potentials and the reasons determining its appearance require additional studies (see Appendix).

Figure 4 represents total voltammograms of the H_2O_2 reduction on a rotating disk GC/PEDOT/Au electrode in 0.2 M PBS at different H_2O_2 concentrations (5×10^{-4}–5×10^{-3} M). An increase of the H_2O_2 concentration in the bathing solution causes a rise of the total limiting current related to the H_2O_2 electroreduction. This limiting current is almost proportional to the H_2O_2 concentration, since its value extrapolated on the zero concentration of H_2O_2 is also close to zero (see insert to Fig. 4). This allows one to think that, at short times of gold deposition (deposition duration 60 s), the contribution of the currents related to the hydrogen generation on gold particles (i.e., the background currents mentioned above) is rather small and can hardly be taken into account, when the total limiting current is discussed. However, if the amount of gold deposited into PEDOT film is increased, the contribution of such process to the measured current might rise significantly, as will be shown below.

We studied the influence of gold loading into PEDOT polymer matrix on the cathodic wave of the hydrogen peroxide reduction. The time of gold deposition from a 1×10^{-3} M $HAuCl_4$ solution was in the range of 60–720 s. Each time, a new PEDOT film synthesized under standard conditions was used. Voltammetric curves of the synthesized PEDOT/Au films with different Au loadings are represented in Fig. 5 for the case of a 0.2 MPBS solution with addition of 1×10^{-3} M H_2O_2. An increase of the amount of gold loaded into the films led to a shift of the half-wave potential of the overall cathodic wave to more positive values and its gradual splitting into two waves (Fig. 5). These facts point to some acceleration of the hydrogen peroxide reduction, which in the case of large amounts of gold proceeds predominantly on gold particles. It is also seen that the H_2O_2 reduction wave is well-separated from the second wave of the hydrogen generation on gold particles. Such a separation also reveals an increased contribution of the last process (hydrogen generation from proton-donor species) in these conditions.

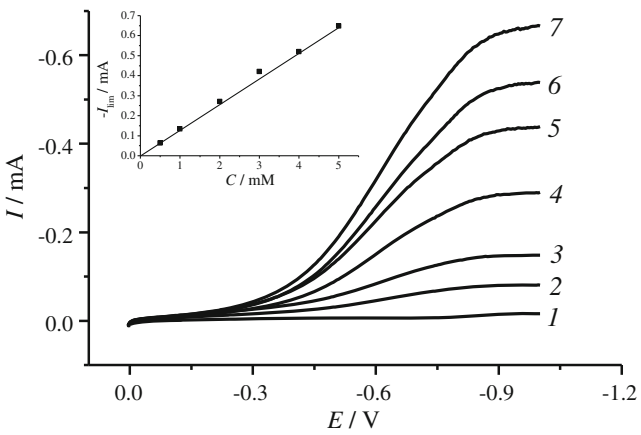

Fig. 4 RDE voltammetry curves for the hydrogen peroxide reduction on composite PEDOT/Au film in PBS solution at different concentrations of H_2O_2, M: *1* 0, *2* 0.5×10^{-3}, *3* 1×10^{-3}, *4* 2×10^{-3}, *5* 3×10^{-3}, *6* 4×10^{-3}, *7* 5×10^{-3} (substrate—GC disk of 0.07 cm^2, *f*=2,500 rpm, scan rate 10 mV s^{-1}, duration of gold loading—60 s). On the inset: calibration plot I_{lim} vs. $C(H_2O_2)$

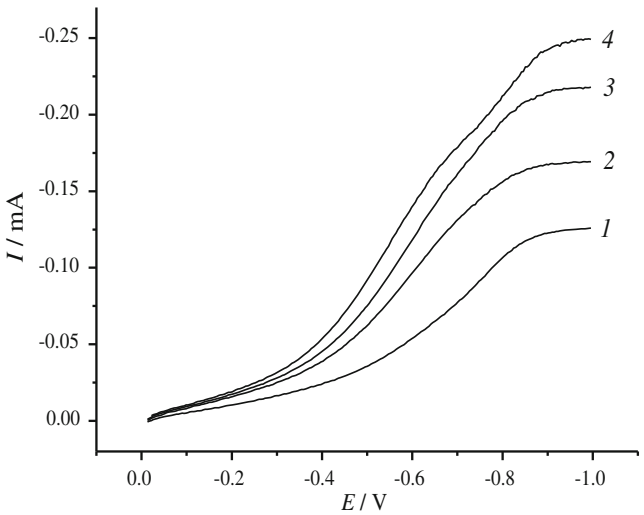

Fig. 5 RDE voltammetry curves for the hydrogen peroxide reduction on composite PEDOT/Au film in PBS solution plus 1×10^{-3} M H_2O_2. Durations (s) of gold loading from solution of $1\times10^{-3}M$ $HAuCl_4$+ 0.1 M H_2SO_4 are as follows: *1* 60, *2* 150, *3* 240, *4* 720

As the first approximation, additivity and independence of currents of the above parallel electrode processes can be assumed, which allows one to estimate partial currents of the hydrogen peroxide reduction on gold particles. A concrete way of such estimation can be explained with the help of data given in Fig. 3, where experimental voltammetric curves are represented for both a composite (PEDOT/Au) film and a pristine (PEDOT) one in the presence of H_2O_2, as well as a background curve of the same composite film in the absence of H_2O_2. To obtain a partial voltammogram of the H_2O_2 reduction on gold particles (curve 5 of Fig. 3), currents corresponding to the hydrogen generation on gold particles (curve 3 of Fig. 3) and those of the H_2O_2 reduction on the surface of the pristine film (curve 2 of Fig. 3) were subtracted from the registered total currents (curve 4 of Fig. 3).

Here, we ought to point out some restrictions of similar estimations. It should be clear that, in case of composite films, such estimations presume the occupancy of the polymer surface with gold particles to be small. Indeed, the rate of the hydrogen peroxide reduction on the free polymer surface should not change significantly under transition from a pristine film to a composite one, assuming that the film/solution interface of the composite film is not practically occupied with metal particles. This condition is obviously fulfilled only at low duration τ of gold's loading into the films. However, the proposed estimation seems to be right for all the durations used, at least in the first approximation, if the region of relatively low total currents is analyzed by the indicated mean. Indeed, in the range of total currents being relatively far from their limiting values, the rate of the H_2O_2 reduction on the free polymer surface is substantially lower than that of the same process on the surface of gold clusters due to the indicated great difference in the half-wave potentials of these processes (see above). The same premise applies to the contribution of currents resulting from the hydrogen generation (from proton-donor species) on gold clusters. As regards the currents close to the limiting values, the errors introduced with the above subtraction procedure might substantially decrease the determined partial rate of the H_2O_2 reduction on gold clusters in the general case of comparable free and occupied film surfaces. Such a decrease should result from the evident fact that the same species are consumed in the parallel processes considered (hydrogen peroxide species and hydrogen ions). It is clear that, in the case of the simultaneous occurrence of all the processes, the surface concentrations of these particles must be smaller than those corresponding to a separate process, the closer the total currents are to their limiting values. Taking these circumstances into account, let us discuss the results obtained using the above approximation.

Calculated partial voltammetric curves of the H_2O_2 reduction on gold particles of PEDOT/Au films are shown in Fig. 6 for different amounts of loaded gold. As it is seen, small current maxima arise on such partial voltammograms at high gold loadings (see Fig. 6, curve 5 and especially curve 6). This most likely results from the fact that, during the used subtraction of background currents (hydrogen peroxide reduction on the pristine films and hydrogen generation (in the absence of H_2O_2) on composite ones), we did not account for the indicated decreases of such currents at the simultaneous proceeding of all the processes. One can also see, that at long durations of gold loading, partial voltammograms appear practically to be coinciding and their half-wave potential becomes close to that of the H_2O_2 electroreduction on a polycrystalline gold electrode (about −0.53 V).

Based on the partial curves of Fig. 6, the Tafel plots of E vs $\log[j/(j_d-j)]$ corrected for a mass transfer were constructed for the hydrogen peroxide reduction on the gold particles' surface of composite films (see Fig. 7). As one would expect from what has been said above, linear parts of these semi-logarithmic dependences are observed in the main range of the electrode potentials, where the calculated currents are not close to the determined limiting current values. Tafel slope values b_k of linear parts of all the curves were in the range of 0.21–0.24 V/dec. From the obtained slopes ($b_k=2.303RT/\alpha' F$), the apparent transfer coefficient of the cathodic process in question was estimated as quantity $\alpha'=0.24$–0.28.

The half-wave potentials for the partial waves of the hydrogen peroxide reduction on gold particles obtained

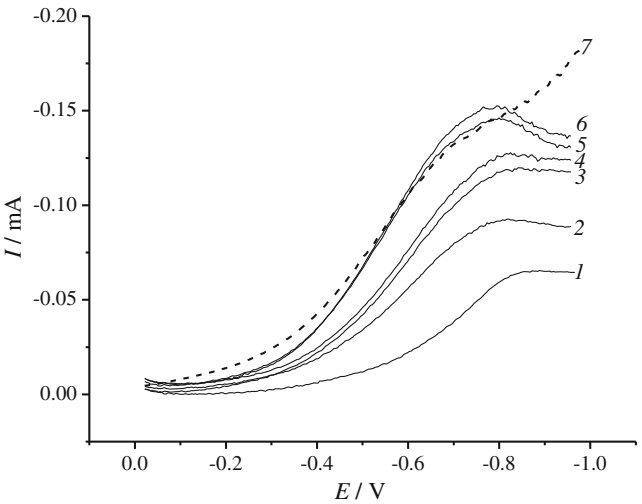

Fig. 6 Partial RDE voltammetry curves for the hydrogen peroxide reduction on Au particles in PBS solution plus 1×10^{-3} M H_2O_2. Durations (s) of gold loading from solution of 1×10^{-3}M $HAuCl_4$+ 0.1 M H_2SO_4 are as follows: *1* 60, *2* 150, *3* 240, *4* 330, *5* 560, *6* 720. *Curve 7* corresponds to the hydrogen peroxide reduction on a polycrystalline gold electrode in the same solution

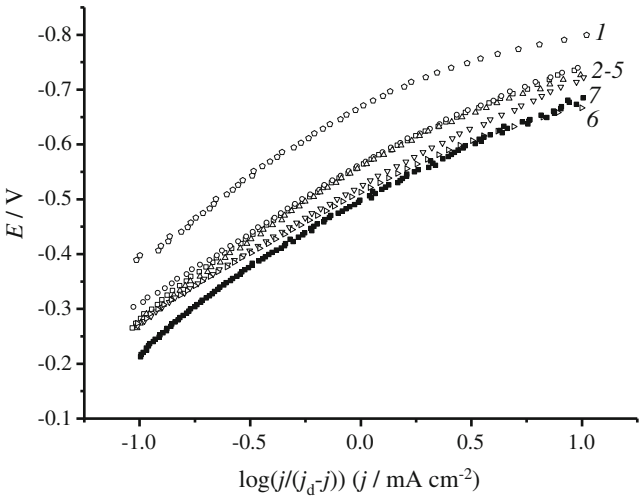

Fig. 7 Mass-transfer corrected Tafel plots for the hydrogen peroxide reduction on Au particles in PBS solution plus 1×10^{-3} M H_2O_2 at different durations of gold loading, *s*: *1* 60, *2* 150, *3* 240, *4* 330, *5* 560, *6* 720. *Curve 7* corresponds to the polycrystalline gold electrode

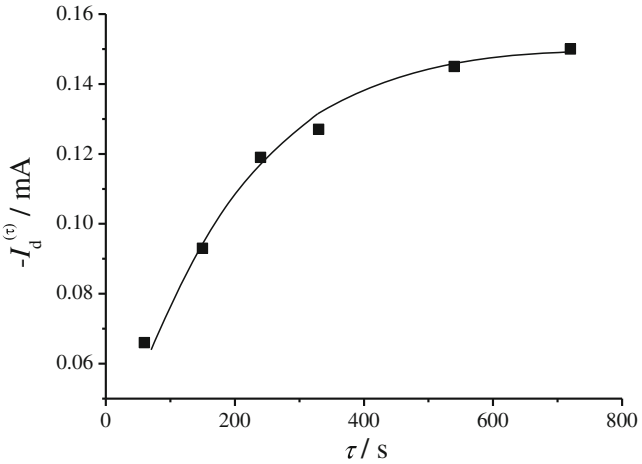

Fig. 8 Partial limiting current $I_d^{(\tau)}$ as a function of duration τ of gold loading

from the dependencies of Fig. 7 are sufficiently close: the values of such potentials observed in case of large duration τ of gold deposition are in the range of −0.54 to −0.60 V. A more substantial deviation of the half-wave potential from the above values is observed only at a short time of gold deposition (60 s). This might be explained by errors in calculations in cases of comparable contributions of the rates of the hydrogen peroxide reduction on gold particles (PEDOT/Au) and the hydrogen evolution on the same electrode in the absence of H_2O_2.

In the case of a polycrystalline gold electrode (Fig. 7) slope b_k of the linear part of the $E[\log(j/(j_d - j))]$-dependence occurs equal to 0.23 V/dec, i.e. it is close to that obtained for the hydrogen peroxide electroreduction on gold particles of PEDOT films. As a consequence, the apparent transfer coefficient value $\alpha'=0.26$ appears to be practically the same, as that was calculated for the case of gold clusters of the composite films.

Figure 8 shows the limiting current values of the H_2O_2 reduction in function of duration τ of gold deposition into PEDOT films. As it is seen from Fig. 8, at relatively short deposition durations, limiting currents increase in proportion to the amount of gold deposited into PEDOT. However, with the further increase of such durations, the limiting currents asymptotically tend to some constant value. Such maximum value is reached at the gold deposition time being in the range of 540–720 s. The observed phenomenon evidently results from a gradual transition from a small active surface of gold particles acting as separate microelectrodes at their low contents in PEDOT films to the conditions of mass-transfer of reacting particles within the bathing electrolyte when increasing the amount of gold in the composite film [45].

If this is the case, the estimated maximum current density should satisfy the Levich equation:

$$I_d = -zFDC_O{}^0/\delta(\omega) = -0.62zFD^{2/3}\nu^{-1/6}\omega^{1/2}C_0 \qquad (1)$$

Here, D, ν, and ω are the diffusion coefficient of tested particles (here, hydrogen peroxide ones), the kinematic viscosity of the used solution, and the angular rotating velocity ($\omega=2\pi f$, where f, the frequency of rotation, rpm), respectively; C_0, the volume concentration of tested particles; z (here, $z=2$) and F, the number of electrons transferred in an elementary act and the Faraday number, correspondingly. Using the limiting current values achieved at large durations of gold deposition (540–720 s), we constructed the dependence of such currents on the square root of rotating velocity. The dependence occurs to be strictly proportional to $\omega^{1/2}$ which means that the Levich equation is fulfilled, at least in respect to the angular velocity (see also further text concerning curve 1 of Fig. 9). At the same time, the diffusion coefficient of H_2O_2 calculated for different rotation rates was equal to 1.1×10^{-5} cm^2 s^{-1}, which is in agreement with the data published in [38]. Thus, in the presence of large amounts of gold in PEDOT/Au films, the H_2O_2 transport to the visible electrode surface is actually limited by diffusion of hydrogen peroxide particles in the adjacent electrolyte.

It also occurs that the calculated limiting currents of the H_2O_2 reduction depend on the rotating velocity even if the gold deposition times are so short (for example, 60 s), that the maximum limiting current is not achieved at such conditions. Quantitative features of such a dependence are revealed in a more explicit form if one uses the Koutecky–Levich coordinates of $1/I_d^{(\tau)}$ vs $\omega^{-1/2}$, where $I_d^{(\tau)}$ is the total limiting current recorded at the gold deposition time equal

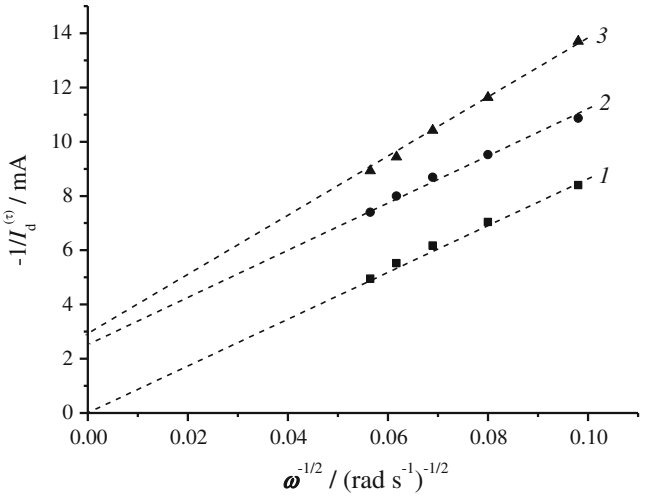

Fig. 9 Koutecky–Levich plots of $1/I_d^{(\tau)}$ vs. $\omega^{-1/2}$ for the hydrogen peroxide reduction on composite PEDOT/Au film in PBS solution plus 1×10^{-3} M H_2O_2 at different durations of gold loading from solution of 1×10^{-3} M $HAuCl_4$, *s*: *1* 720, *2* 60 (partial currents), *3* 60. *Curve 2* represents partial limiting currents of H_2O_2 reduction on gold particles

to τ (see curve 2 of Fig. 9 and legend to it). As it is seen, these dependences appear to be linear and their initial segments (i.e., values of $1/I_d^{(\tau)}$ extrapolated on $\omega=\infty$) substantially deviate from the origin of coordinates at short durations τ. However, they tend to zero at large durations τ, i.e., the limit that corresponds to the diffusion limiting current strictly proportional to $\omega^{1/2}$, as indicated above. One can assume those extrapolated values to be some kinetic components of the current, which are independent of the rotation velocity. However, this supposition does not reply on the evident question: "what is the nature or an origin of such components?" The simplest consideration given in the Appendix to this paper allows one to get the desired answer.

By referring the readers to the Appendix, we should note here that the simultaneous H_2O_2 reduction on both the surface of the gold clusters and the composite film free of the clusters is accounted for in a more exact manner in the Appendix than the subtraction procedure used above. In particular, it is shown there that the total limiting current of both processes (i.e., the measured limiting current, $2FI^{(1)}$, in the notations of the Appendix), if one ignores its relatively small constituent resulting from the hydrogen generation on gold clusters, should satisfy Eq. A.16, namely

$$-\frac{1}{2FI^{(1)}}=\frac{1}{2FC_0\left[\pi D\sum_{i=1}^{m}n_i\gamma_i r_i+\rho C_x(\infty)(A-\pi\Sigma_2)\right]}+\frac{\delta}{2FC_0DA_0} \tag{2}$$

At the same time, the partial rate of the H_2O_2 reduction on the gold clusters' surface ($-1/2FJ_f^{(1)}$ in the same notations) is as follows (see also Eq. A.15)

$$-\frac{1}{2FJ_f^{(1)}}=\frac{1}{2F\pi DC_0\sum_{i=1}^{m}n_i\gamma_i r_i}+\left(\frac{\delta}{2FC_0DA_0}1\right)\left[1+\frac{\rho C_x(\infty)(A-\pi\Sigma_2)}{\pi D\sum_{i=1}^{m}n_i\gamma_i r_i}\right] \tag{3}$$

Here, $\pi\Sigma_2=\pi\sum_{i=1}^{m}n_i\sigma_i r_i^2$ is the surface occupied by metal clusters of different radii r^i on the film/solution interface of total area A; n_i and σ_i are the number of clusters of the *i*th kind (i.e. clusters having the radii equal to r_i) and the factor characterizing a partial immersion of the *i*th clusters into the film, respectively; γ_i is a factor of such value, that product $\pi\gamma_i r_i^2$ represents the *i*th cluster's surface not immersed into the film and, hence, accessible to hydrogen peroxide species; A_0, the visible surface of the film; ρ, the heterogeneous rate constant of the H_2O_2 reduction on the film surface free of metal clusters; $C_x(\infty)$ is an empirical factor that should be introduced to account for the existence of limiting currents of the above reaction (for details see Appendix).

A few words should be said here to comment the physical meaning of the above equations of the Koutecky–Levich type. As was in essence mentioned earlier, the observed rise of the limiting currents with increasing the gold content in modifying PEDOT films results from the gradual transition from separate gold microelectrodes, which act independently in the limit of a small gold content, to their functioning at the conditions when diffusion layers surrounding separate gold clusters completely overlap each other. The hydrogen peroxide amounts consumed in the last case must obviously be greater than those of the first limit (one can imagine that only one cluster exists in such limit). This means an apparent acceleration of the electroreduction process, though its rate on separate clusters in reality lowers (with increasing their total number) due to relevant decreases of surface concentration $C(0)$ of tested particles (see Appendix). In other words, the limiting currents at intermediate gold contents can be increased account for intensive convection up to their values given by the denominators of the first terms of the right parts of Eqs. 2 and 3, which corresponds to the case of $C(0)=C_0$. These peculiarities of the electroreduction are reflected by the above equations. Their concrete forms are rather complicated as compared to the traditional one, since the H_2O_2 electroreduction proceeds simultaneously on the film surface and the gold clusters one.

From the Koutecky–Levich representations of the total and partial limiting currents given above (i.e., Eqs. 2 and 3, correspondingly), it can be deduced that both the intercepts and the slopes (with respect to $\omega^{-1/2}$) of these dependences should be different. The intercept of the reverse partial current $(-1/2FJ_f^{(1)})$ is nothing else but the reverse sum over all limiting currents $2F\pi DC_0 n_i \gamma_i r_i$ to all the ith clusters possessing surfaces $\pi\gamma_i r_i^2$, which are accessible to hydrogen peroxide particles. As to the reverse total current, its intercept is also a reverse sum that, beside the sum defined previously, includes maximum current $2F\rho C_x(\infty)C_0(A-\pi\sum_2)$ of the H_2O_2 reduction on film surface $(A-\pi\sum_2)$ free of metal clusters. One can also see from the discussed equations that slope $\mathrm{d}\left(-1/2FJ_f^{(1)}\right)/\mathrm{d}\left(\omega^{-1/2}\right)$ must exceed slope $\mathrm{d}(-1/2FI^{(1)})/\mathrm{d}(\omega^{-1/2})$ of the reverse total current by $\left[1+\frac{\rho C_x(\infty)(A-\pi\Sigma_2)}{\pi D\sum_{i=1}^{m} n_i\gamma_i r_i}\right]$ times, i.e., their difference should be the greater the higher the contribution of the H_2O_2 reduction on the polymer surface free of metal clusters to the total current. At the same time, the above slope of the reverse total current should be the same as that which occurs for the reverse diffusion limiting current:

$$\mathrm{d}\left(-1/2FI^{(l)}\right)/\mathrm{d}\left(\omega^{-1/2}\right) \equiv \mathrm{d}(-1/2FI_d)/\mathrm{d}\left(\omega^{-1/2}\right) = 1.61D^{-1/3}\nu^{1/6}C_0{}^{-1} \quad (4)$$

The peculiarities of the discussed dependences can be used to test whether the approach applied in this work is valid. To do this at the present state of the research, one should evidently equate the experimental values of the limiting partial and total currents to currents $2FJ_f^{(1)}$ and $2FI^{(l)}$, respectively. The corresponding results are represented in Fig. 9 (see legend to the figure). As it is seen, the slope of the dependence of the reverse partial current on $\omega^{-1/2}$ (curve 3) actually exceeds that of the reverse total current (curve 2). At the same time, the slope of curve 2 has practically the same value as the value inherent to curve 1, which corresponds to the limiting currents achieved at large durations τ of gold loading. As established earlier, the last current values satisfy the Levich equation. We can therefore say that the second requirement of the theory, namely Eq. 4, is fulfilled. Finally, it should be pointed out that the intercept of *curve 1* is greater than that of curve 2 and their ratio is close to the observed ratio of the slopes of these curves. Such type of correlation between the compared parameters must be observed according to Eqs. (2, 3) and, hence, the obtained experimental results are in accord with the main theoretical consequences.

One could use more general Eqs. A.12, A.13, and A.14 of the Appendix to estimate rate constants k_i and ρ, but we consider such attempts to be premature. Indeed, the above partial currents were determined only in the first approximation. Their more exact estimations are possible but need additional studies (see Appendix). We therefore plan to perform a more detailed comparison between experimental and theoretical results in the future.

Conclusion

It is established that the hydrogen peroxide electroreduction on composite PEDOT/Au films takes place not only at the gold clusters' surface but also the film surface free of metal inclusions. Division of the measured currents of the total reduction into its constituents related to the partial processes is performed in the first approximation, namely assuming their additivity and independence. This supposition is in a great extent justified by the fact that the H_2O_2 reduction on gold clusters begins at the electrode potentials, being more positive (about 0.2 V), than those corresponding to the reduction on the film surface free of clusters. Such a division shows the absence of a significant catalytic activity (with respect to the reaction under consideration) of gold clusters as compared to polycrystalline gold electrodes. The rate of the observed parallel electroreduction occurs dependent on the amount of gold loaded into the films. It is shown that the changes of the total and partial limiting currents obtained at varying rotation velocity and gold loadings of PEDOT/Au modified RDE are in accord with theoretical predictions based on quantitative simulations of the process in question.

Acknowledgments The authors are thankful to Drs. Anton Bondarenko, Oleg Vyvenko, and Evgeny Ubyivovk for the help we have received during joint SEM and TEM measurements. We also thank the Russian Foundation for Basic Research for financial support of this work (grants ##10-03-00793, 10-08-00895). The work was also supported by research grant No. 12.38.15.2011 of the St. Petersburg State University.

Appendix

We shall, in essence, use here the approach of Ref. [45] devoted to quantitative simulations of charge transfer processes in conducting polymer films containing metal clusters of small radii. As it was done in the cited paper, we firstly remind the readers that, in the case of microelectrodes settled far apart, the following radial distribution of particles participating in an electrode reaction on the surface of a separate cluster is valid:

$$C_i(r) = r_i^2 j_i/Dr + C_0 \quad (A.1)$$

Here, $C_i(r)$ is a local concentration of such particles at distance r from the center of the spherical cluster

considered; r_i, the cluster radius; $j_i = -D\mathrm{d}C_i(r)/\mathrm{d}r|_{ri}$ is the flow of tested particles (here, hydrogen peroxide ones) per unit surface of the cluster; symbol $\mathrm{d}C_i(r)/\mathrm{d}r|_{ri}$ is assigned to the value of the radial derivative at $r = r_i$; C_0, the bulk concentration of tested particles in the medium surrounding the clusters. Assuming an electrode reaction (not obligatory the considered electroreduction of hydrogen peroxide particles) is irreversible and satisfying the first order kinetics, one can apply the usual expression for flux j_i, namely

$$j_i = -k_i(E)C_i(r_i), \tag{A.2}$$

where $k_i(E)$ is the rate constant dependent of electrode potential E. As it follows from Eqs. (A.1 and A.2), flux j_i can be written in two forms:

$$j_i = -D[C_0 - C_i(r_i)]/r_i \text{ and } j_i = -k_i(E)C_0/[1 + k_i(E)r_i/D] \tag{A.3}$$

From the first equation it is clear that radius r_i plays the role of the diffusion layer surrounding the cluster of such radius. As one could see, the radii of gold clusters determined above (see part 3.1) do not exceed 100 nm, i. e. they are much smaller than diffusion layer thickness $\delta = 1.61D^{1/3}\nu^{1/6}\omega^{-1/2} \geq 10^{-3}$ cm at rotating velocities ω used in this work. This, in essence, means that the surface concentration of tested particles near the electrode used, $C(0)$, should replace bulk concentration C_0 in the above equations. Indeed, gradients $\mathrm{d}C_i(r)/\mathrm{d}r$ near the ith clusters (i.e. clusters having the radius equal to r_i) must turn to zero at distances $r > 2r_i$; i.e. concentration $C(0)$ should, actually, be considered as the bulk concentration for the medium surrounding the ith clusters. If so, the total flow of tested particles, J_f, summarized over surfaces $n_i\gamma_i\pi r_i^2$ of all the clusters, where $\gamma_i \leq 4$ is a part of the ith clusters' surface accessible to tested particles (in the meaning of proceeding their electrochemical reaction) and n_i is the number of clusters of the ith kind on the film/solution interface, can be written as follows

$$J_f = -\pi C(0)\sum_{i=1}^{m}\frac{n_i\gamma_i r_i^2 k_i(E)}{1 + \frac{k_i(E)r_i}{D}}, \tag{A.4}$$

where m is the total number of different (ith) kinds of clusters, i.e., clusters having different values r_i of their radii. Let us assume that tested particles react also with either reduced (as in the case of the reaction $H_2O_2 + 2e \rightarrow 2OH^-$) or oxidized film fragments of concentration $C_x(E)$, and total flow I_f of such a process to the film surface free of the included metal clusters is given by the equation

$$I_f = -\rho C(0)C_x(E)\left(A - \pi\sum_{i=1}^{m} n_i\sigma_i r_i^2\right) \tag{A.5}$$

Here, A is the above mentioned total surface of the film/solution interface; $n_i\sigma_i\pi r_i^2$ is the surface occupied by clusters of the ith kind at the same interface; ρ is the rate constant that might in principle be dependent on the electrode potential.

Here, we must do some premise concerning peculiarities of pristine PEDOT films used in this work. At high negative potentials ($-0.4\ \mathrm{V} > E > -1.1\ \mathrm{V}$) corresponding to the hydrogen peroxide electroreduction, these films should be in a non-conducting state. The latter obviously corresponds to a neutral form of all the fragments of polythiophene chains of the film, which in particular means that concentration $C_x(E)$ should be practically constant at these conditions. At least in scope of the so-called homogeneous film model [46], this means that, within the indicated range of E, the electric potential of the film/solution interface should be independent of the electrode potential. In other words, one can put heterogeneous rate constant ρ of the H_2O_2 reduction on the PEDOT film/solution interface to be some constant and, hence, consider the rate of the process as an unchanged quantity at the indicated potential values. Meanwhile, substantial changes in this rate are observed in the electrode potential range from −0.4 V up to −0.9 V (see curve 3 of Fig. 3). Now, it remains unclear what factors are responsible for the observed phenomenon, which obviously needs the further research. We will therefore define quantity $C_x(E)$ as a factor, the value of which tends to constant $C_x(\infty)$ in the limit of high negative potentials E, as it takes place in reality.

The total flow of tested particles to the modified electrode in question, I, should satisfy the mass conservation condition:

$$I = J_f + I_f = -DA_0[C_0 - C(0)]/\delta \tag{A.6}$$

The latter gives the evident expression for concentration $C(0)$

$$C(0) = C_0[1 - (J_f + I_f)/I_d], \tag{A.7}$$

where $I_d = -0.62A_0D^{2/3}\nu^{-1/6}\omega^{1/2}\ C_0$ is the limiting diffusion flow to the rotating disk electrode, the visible surface of which equals $A_0 \leq A$. Substituting Eqs. A.7 into Eqs. A.4 and A.5 leads to a system of linear algebraic equations with respect to functions J_f and I_f unknown so far. Solving such system, one can obtain the folowing expressions for these flows:

$$J_f = -\pi C_0\Sigma_1\left(1 + \frac{\delta}{DA_0}(\pi\Sigma_1 + \rho C_x(E)(A - \pi\Sigma_2))\right)^{-1} \tag{A.8}$$

$$I_f = -\rho C_0C_x(E)(A - \pi\Sigma_2)\left(1 + \frac{\delta}{DA_0}(\pi\Sigma_1 + \rho C_x(E)(A - \pi\Sigma_2))\right)^{-1}, \tag{A.9}$$

where

$$\sum\nolimits_1 = \sum_{i=1}^{m} \frac{n_i \gamma_i r_i^2 k_i(E)}{1 + \frac{k_i(E) r_i}{D}}, \sum\nolimits_2 = \sum_{i=1}^{m} n_i \sigma_i r_i^2 \tag{A.10}$$

As to total flow $I = J_f + I_f$, the corresponding expression is as follows

$$I = -\frac{\pi C_0 \Sigma_1 + \rho C_0 C_x(E)(A - \pi\Sigma_2)}{1 + \frac{\delta}{DA_0}(\pi\Sigma_1 \rho C_x(E)(A - \pi\Sigma_2))} \tag{A.11}$$

From the expressions derived above, a series of conclusions can be extracted. First, as mentioned earlier (see part 3.2), flow I_f (in the paper context, the rate of the hydrogen peroxide electroreduction on the film/solution interface free of metal clusters) must differ from flow I_f^0 of these species to the pristine film. Indeed, such flow should be equal to:

$$I_f^0 = -\rho C_0 C_x(E) A \{1 + \delta \rho C_x(E) A / DA_0\}^{-1}, \tag{A.9'}$$

as it follows from Eqs. A.9 at $\sum_1 = \sum_2 = 0$, which is the evident condition of the absence of metal clusters. This means that the performed subtraction of flow I_f^0 from total flow I (see part 3.2) actually leads to some inaccuracy of such determinations of partial flow J_f to the surface of metal clusters. It is obvious that the error resulting from such subtraction should be at its maximum when the total flow I is close to its limiting values $I_{lim}(\tau)$ dependent on gold loading duration τ, as shown above. This, obviously, implies that limiting values $J_{lim}(\tau)$ of flows $J_f^{(s)}$ determined at such subtraction are smaller than those, which take place in reality. Such decreases of $J_{lim}(\tau)$ (as compared to real flows) should lead to noticeable deviations of semi-logarithmic dependences of $\log\{J_f^{(s)} / \left[J_{lim}(\tau) - J_f^{(s)}\right]\}$ vs E from linear ones in the range of flows $J_f^{(s)}$ comparable with $J_{lim}(\tau)$, i.e. the phenomenon observed in reality (see Fig. 7). As to smaller flows $J_f^{(s)}$, the corresponding errors and, hence, the above deviations from linearity should practically be insignificant, since the wave of the hydrogen peroxide reduction on the film/solution interface is settled at significantly more negative potentials (about 0.2 V, see the main text) than the wave of the same process on the metal clusters' surface. This was the main reason, why we have used the discussed subtraction procedure in this work.

To elucidate other conclusions followed from the above derivations, one should use the Koutecky–Levich representation of the flows in question:

$$-\frac{1}{J_f} = \frac{1}{\pi C_0 \Sigma_1} + \frac{\delta}{DA_0 C_0}\left(1 + \rho C_x(E)\frac{(A - \pi\Sigma_2)}{\pi\Sigma_1}\right) \tag{A.12}$$

$$-\frac{1}{I_f} = \frac{1}{\rho C_x(E) C_0 (A - \pi\Sigma_2)} + \frac{\delta}{DA_0 C_0}\left(1 + \frac{\pi\Sigma_1}{\rho C_x(E)(A - \pi\Sigma_2)}\right) \tag{A.13}$$

$$-\frac{1}{I} = \frac{1}{C_0(\rho C_x(E)(A - \pi\Sigma_2) + \pi\Sigma_1)} + \frac{\delta}{DA_0 C_0} \tag{A.14}$$

As one can see, only slope $\mathrm{d}(-1/I)/\mathrm{d}\omega^{-1/2})\big|_{E = \mathrm{Const}}$ must coincide with that of the dependence of $-1/I_d$ as a function of $\omega^{-1/2}$, where I_d is the limiting diffusion flow to RDE. Such slopes of the dependences given by Eqs. A.12 and A.13 should exceed the above mentioned ($\mathrm{d}(-1/I)/\mathrm{d}(\omega^{-1/2})$) by $[1+\rho C_x(E)(A-\pi\sum_2)/\pi\sum_1]$ and $[1+\pi\sum_1/\rho C_x(E)(A-\pi\sum_2)]$ times, correspondingly. It is also seen that the intercepts of all the dependences are different. If, in the case of Eqs. A.12 and A.13, they are determined by values of the corresponding partial flows (without introduced mass-transfer corrections), in case of total flow I (i.e., Eqs. A.14) the intercept is reversed in proportion to the sum of such flows.

Turning finally to the case of limiting flows, we indicate that, at high $|E|$, factor $C_x(E)$ should take some maximum value $C_x(\infty)$; see above). In the same limit, terms $n_i\gamma_i r_i^2 k_i(E)/[1 + k_i(E) r_i/D]$ of sum $\sum_1$ must obviously tend to $Dn_i\gamma_i r_i$, since $k_i(E) = k_i^0 \exp(-\alpha FE/RT)$, where transfer coefficient α is about 0.24, as was established (see part 3.2). Taking these indications into account, one obtains the following expressions for reverse limiting flows $1/J_f^{(1)}$ and $1/I^{(1)}$:

$$-\frac{1}{J_f^{(1)}} = \frac{1}{\pi D C_0 \sum_{i=1}^{m} n_i \gamma_i r_i} + \frac{\delta}{DA_0 C_0}\left(1 + \rho C_x(\infty)\frac{(A - \pi\Sigma_2)}{\pi D \sum_{i=1}^{m} n_i \gamma_i r_i}\right) \tag{A.15}$$

$$-\frac{1}{I^{(1)}} = \frac{1}{C_0\left(\pi D \sum_{i=1}^{m} n_i \gamma_i r_i + \rho C_x(\infty)(A - \pi\Sigma_2)\right)} + \frac{\delta}{DA_0 C_0} \tag{A.16}$$

It remains to add that in the limit of large durations of gold loading, one can consider numbers n_i to be of so great values, that the intercepts of the above dependences become equal to zero. The same concerns the ratio of $\rho C_x(\infty)(A-\pi\sum_2)/\pi D\sum n_i\gamma_i r_i$. Thus, in this limit, both flows should tend to the limiting diffusion flow, as observed in reality. Ignoring the mentioned errors in our experimental determinations of flows J_f and I (see the main text), we used the above equations to treat the experimental results.

References

1. Kim BY, Cho MS, Kim YS, Son Y, Lee Y (2005) Synth Met 153:149–152

2. Selvaganesh S, Mathiyarasu J, Phani KLN, Yegnaraman V (2007) Nanoscale Res Lett 2:546–549
3. Kim SY, Lee Y, Cho MS, Son Y, Chang JK (2007) Mol Cryst Liq Cryst 472:201–207
4. Zanardi C, Terzi F, Pigani L, Heras A, Colina A (2008) Electrochim Acta 53:3916–3923
5. Terzi F, Zanardi C, Martina V, Pigani L, Seeber R (2008) J Electroanal Chem 619–620:75–82
6. Mathiyarasu J, Senthilkumar S, Phani KLN, Yegnaraman V (2008) Mater Lett 62:571–573
7. Harish S, Mathiyarasu J, Phani KLN (2009) Mater Res Bull 44:1828–1833
8. Manesh KM, Santhosh P, Gopalan A, Lee KP (2008) Talanta 75:1307–1314
9. Kumar SS, Mathiyarasu J, Phani KL (2005) J Electroanal Chem 578:95–103
10. Li X, Li Y, Tan Y, Yang C, Li Y (2004) J Phys Chem B 108:5192–5199
11. Pogulaichenko NA, Hui S, Tolstopjatova EG, Malev VV, Kondratiev VV (2009) Russ J Electrochem 45:1176–1182
12. Kumar SS, Kumar CS, Mathiyarasu J, Phani KLN (2007) Langmuir 23:3401–2408
13. Lu G, Li C, Shen J, Chen Z, Shi G (2007) J Phys Chem C 111:5926–5931
14. Huang X, Li Y, Chen Y, Wang L (2008) Sens Actuators B 134:780–786
15. Xu JJ, Peng R, Ran Q, Xian Y, Tian Y, Jin L (2010) Talanta 82:1511–1515
16. Sekli-Belaidi F, Temple-Boyer P, Gros P (2010) J Electroanal Chem 647:159–168
17. Zanardi C, Terzi F, Seeber R (2010) Sens Actuators B 148:277–282
18. Terzi F, Zanfrognini B, Zanardi C, Pigani L, Seeber R (2011) Electrochim Acta 56:3575–3579
19. Sarma TK, Chowdhury D, Paul A, Chattopadhyay A (2002) Chem Commun 10:1048–1049
20. Hatchett DW, Josowicz M, Janata J (1999) Chem Mater 11:2989–2994
21. Saheb A, Smith JA, Josowicz M, Janata J, Baer DR, Engelhard MH (2008) J Electroanal Chem 621:238–244
22. Li N, Lei T, Liu Y, He Y, Zhang Y (2010) Trans Nonferrous Met Soc China 20:2314–2319
23. Chen Z, Pina CD, Falletta E, Faro ML, Pasta M, Rossi M, Santo N (2008) J Catal 259:1–4
24. Sheffer M, Mandler D (2009) Electrochim Acta 54:2951–2956
25. Hung CC, Wen TC, Wei Y (2010) Mater Chem Phys 122:392–396
26. Stoyanova A, Ivanov S, Tsakova V, Bund A (2011) Electrochim Acta 56:3693–3699
27. Chung SM, Paik W, Yeo IH (1997) Synth Met 84:155–156
28. He Y, Yuan J, Shi G, Wu P (2006) Mater Chem Phys 99:253–257
29. Rapecki T, Donten M, Stojek Z (2010) Electrochem Commun 12:624–627
30. Liu YC, Yang KH (2006) Electrochim Acta 51:5376–5382
31. Chen W, Li CM, Chen P, Sun CQ (2007) Electrochim Acta 52:2845–2849
32. Delvaux M, Walcarius A, Demoustier-Champagne S (2004) Anal Chim Acta 525:221–230
33. Erikson H, Jurmann G, Sarapuu A, Potter RJ, Tammeveski K (2009) Electrochim Acta 54:7483–7489
34. Adžić RR, Marković NM (1982) J Electroanal Chem 138:443–447
35. Adzic R, Strbac S, Anastasijevic N (1989) Mater Chem Phys 22:349–375
36. El-Deab M, Ohsaka T (2002) Electrochem Commun 4:288–292
37. Zeis R, Lei T, Sieradzki K, Snyder J, Erlebacher J (2008) J Catal 253:132–138
38. Wang L, Bo X, Bai J, Zhu L, Guo L (2010) Electroanalysis 22:1–7
39. Guo S, Wen D, Dong S, Wang E (2009) Talanta 77:1510–1517
40. Ma L, Ruo Y, Chai Y, Chen S (2009) J Mol Catal B: Enzym 56:215–220
41. Lobyntseva E, Kallio T, Alexeyeva N, Tammeveski K, Kontturi K (2007) Electrochim Acta 52:7262–7269
42. Bobacka J, Lewenstam A, Ivaska A (2000) J Electroanal Chem 489:17–27
43. Bard AJ, Parsons R, Jordan J (1985) Standard potentials in aqueous solutions. Marcel Dekker, New York
44. Eliseeva SN, Ubyivovk EV, Bondarenko AS, Vyvenko OF, Kondratiev VV (2010) Russ J General Chem 80:1143–1148
45. Malev VV, Levin OV (2011) Electrochim Acta 56:3586–3596
46. Malev VV, Levin OV, Vorotyntsev MA (2006) Electrochim Acta 52:133–151